Space Sci Rev (2007) 130: 409–414
DOI 10.1007/s11214-007-9186-2

The Chemical Composition of Interstellar Matter at the Solar Location

Jonathan D. Slavin · Priscilla C. Frisch

Received: 14 February 2007 / Accepted: 4 April 2007 /
Published online: 11 May 2007
© Springer Science+Business Media, Inc. 2007

Abstract The Local Interstellar Cloud (LIC) surrounds the Solar System and sets the boundary conditions for the heliosphere. Using both in situ and absorption line data towards ϵ CMa we are able to constrain both the ionization and the gas phase abundances of the LIC gas at the Solar Location. We find that the abundances are consistent with all of the carbonaceous dust grains having been destroyed, and in fact with a supersolar abundance of C. The constituents of silicate grains, Si, Mg, and Fe, appear to be sub-solar, indicating that silicate dust is present in the LIC. N, O and S are close to the solar values.

Keywords ISM: abundances · ISM: individual (Local Interstellar Cloud)

1 Introduction

The elemental composition of the LIC, which surrounds the Solar System, can be derived from UV absorption line data, but requires models to fill in the gaps in the data. In particular we do not know directly the total H column density along the line of sight. In addition, for several elements, important ionization corrections need to be made to obtain total column densities from the observed ion column densities. We have created detailed models for the ionizing radiation field and used the radiative transfer code Cloudy (Ferland et al. 1998) to calculate the ionization in the LIC. These models provide the composition of interstellar neutrals that flow into the heliosphere and form the parent population of pickup ions (PUIs) and anomalous cosmic rays (ACRs).

J.D. Slavin (✉)
Harvard-Smithsonian Center for Astrophysics, 60 Garden Street, MS 83, Cambridge, MA 02138, USA
e-mail: jslavin@cfa.harvard.edu

P.C. Frisch
Department of Astronomy & Astrophysics, University of Chicago, 5460 South Ellis Avenue, Chicago, IL 60637, USA

2 Data

Gry and Jenkins (2001) present GHRS and IMAPS data for the line of sight towards ϵ Canis Majoris. This absorption line dataset is notable for its completeness, including lines of Mg I, Mg II, C II, C II*, N I, O I, S II, Si II, Si III, and Fe II for the LIC velocity component. We use the LIC component at 17 km s^{-1} (Table 2 of Gry and Jenkins 2001) for this analysis. In this work we concentrate on this one line of sight as a means of putting constraints on our models that predict the boundary conditions of the heliosphere. Datasets for lines of sight to other nearby stars, e.g. η UMa, Capella, do exist, though most are less complete in terms of the number of detected lines. We will present analyses of more lines of sight in future papers.

3 Model Parameters

There are several important parameters for our photoionization models that are either not directly constrained or constrained poorly by observations:

- total H I column density, N(H I)
- temperature of the hot gas of the Local Bubble, T_h
- total H density at the outer edge of the cloud, n(H)
- the cloud magnetic field, B_0

In our models we explore values of N(H I) = (3–4.5) $\times$ 10^{17} cm^{-2}. A significant fraction of the ionizing radiation field in our models comes from diffuse soft X-ray/EUV emission generated in the hot gas of the Local Bubble. The temperature of that hot gas is uncertain, which affects the spectrum of the emission. Observations of the broad band count rates at soft X-ray energies provide some constraints on the spectrum, but the diffuse EUV emission that provides the bulk of the ionizing photons has not been observed. The hot gas temperatures we explore are $\log T_h = 5.9, 6.0, 6.1$. The treatment of the magnetic field in the cloud is simply as an additional pressure term, $P_M \propto B^2$, with the field strength assumed to go as the density (see Slavin and Frisch 2002). Thus a higher field strength implies a higher total pressure in the cloud. In the transition layer between the warm cloud and hot gas where the magnetic pressure falls off sharply the thermal pressure increases to make up the difference. In our initial model grid we use $B_0 = 2$ and 5 μG. The total H density is also an important model input and is constrained indirectly by the observed He^0 density. Our initial model grid used values of 0.218 and 0.273 cm^{-3} (corresponding to total densities of 0.24 and 0.3 cm^{-3}). After calculating an initial grid of 24 models we then calculated a smaller grid of 6 models in which we fixed $\log T_h$ and N(H I) and varied n(H) and B_0 so as to match the observed values of n(He^0) and T(He^0) observed for interstellar neutrals flowing into the heliosphere.

4 Radiation Field

As in Slavin and Frisch (2002) we construct the interstellar radiation field from both directly observed stellar contributions and diffuse emission that is either unobserved or observed at low spectral resolution. The components of the radiation field include:

- EUV (100 Å $< \lambda <$ 912 Å) from nearby B and white dwarf stars,
- Diffuse soft X-rays ($\lambda <$ 100 Å) from hot gas in the Local Bubble and galactic halo,

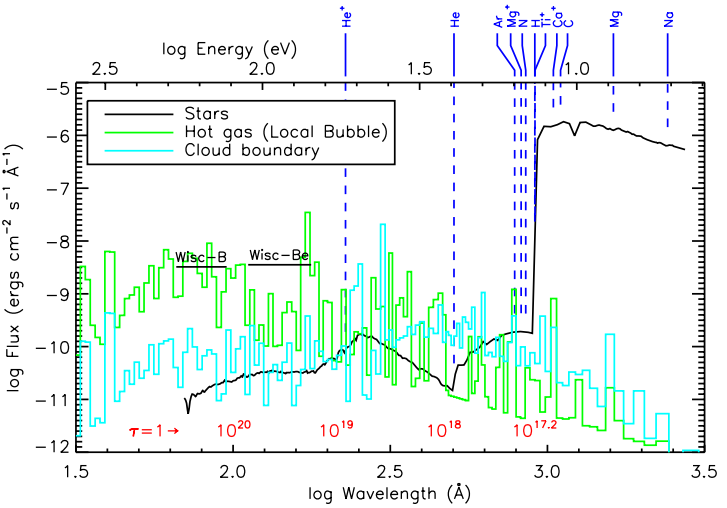

Fig. 1 Background interstellar radiation field responsible for ionizing the LIC. The *black line* is the FUV/EUV flux from stars, the *green line* is a model spectrum for the diffuse emission from hot gas and the *cyan line* is the modeled emission from the evaporative boundary of the cloud. The ionization edges for several important ions are shown in *dark blue*. The wavelength at which the cloud is optically thick for several different column densities is indicated in *red*. The band widths and mean flux levels for the soft X-ray observations by the Wisconsin group are indicated by *horizontal lines*. (Colour figure online)

– FUV (912 Å $< \lambda <$ 3000 Å)—mainly from B stars distributed throughout the galactic disk (Gondhalekar et al. 1980),
– Diffuse EUV emission generated at the boundary of the hot gas in the Local Bubble and the warm (∼6000 K) gas of the LIC.

Figure 1 illustrates the different components of the model radiation field. The stellar FUV strongly dominates the ionization of the low ionization potential ions such as Mg^0, C^0, and Ca^+ whereas the stellar EUV, hot gas emission and cloud boundary flux all play a role in ionizing those ions with ionization potentials above 13.6 eV.

5 Results

We fix the model parameters to get a match to the observed in situ values for $n(He^0) = 0.0151 \pm 0.0015$ and $T(He^0) = 6300 \pm 340$ (Witte 2004). For our best models this results in $B_0 = 0$–3.8 μG and $n_H = 0.21$–0.23 cm^{-3}. The abundances are fixed by the requirement that they fit the observed column densities. Figure 2 summarizes the results for abundances by comparing the derived abundances with solar abundances from Asplund et al. (2005). The relative abundances are plotted against the condensation temperature for the given element, since it is believed that T_C is important for determining the rate at which an element will be incorporated into grains at sites of dust formation. We find that C abundance is very high and S abundance slightly high relative to Solar. On the other hand Fe, Mg and Si, components of silicate dust, all have substantial depletions. N and O have solar or slightly subsolar abundance. Note that our conclusions about C do not rest heavily on our photoionization modeling. As we discuss in Slavin and Frisch (2006), simple assumptions combined with

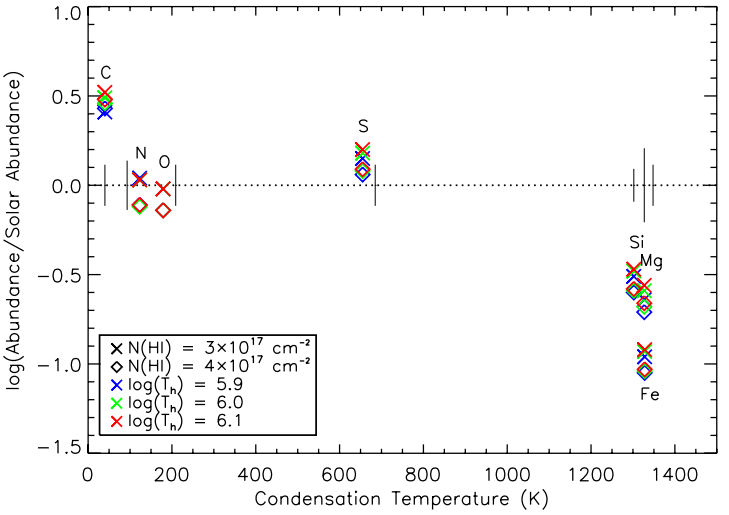

Fig. 2 Abundances derived for the LIC from photoionization models constrained by the Gry and Jenkins (2001) data. Log of the abundance relative to the Solar abundances of Asplund et al. (2005) is plotted vs. the condensation temperature for the element. *Crosses* (×) are for low column density ($N(\mathrm{H\,I}) = 3 \times 10^{17}$ cm^{-2}) models while *diamonds* (◊) are for higher column density models ($N(\mathrm{H\,I}) = 4 \times 10^{17}$ cm^{-2}). The assumed temperature of the hot gas is indicated by the *symbol color*. For these cases B_0 and n_H have been varied so as to match the observed values for T and $n(\mathrm{He}^0)$ at the Solar location (see Slavin and Frisch 2007 for details). The vertical lines indicate the uncertainties in the Solar abundances given by Asplund et al. (Colour figure online)

Table 1 Comparison between Model, In Situ and Interstellar Data

Ratio	Model 26	PUIs corrected for filtration[a]	White Dwarf stars[b]
O^0/N^0	8.3	8.81 ± 2.41	8.6 ± 3.9
O^0/H^0	3.5×10^{-4}	$3.51 \pm 0.01 \times 10^{-4}$	$3.5 \pm 2.2 \times 10^{-4}$
Ar^0/O^0	2.6×10^{-3}	$3.56 \pm 0.17 \times 10^{-3}$	$3.9 \pm 1.4 \times 10^{-3}$ [c]
H^0/He^0	11.8	12.0 ± 1.6	12.8 ± 1.4[d]

[a]The PUI values at the termination shock (Gloeckler and Fisk 2007) have been corrected to interstellar densities using filtration factors of 0.6, 1.0, 0.8, 0.8, and 0.76 for H, He, N, O, and Ar, respectively (Cummings et al. 2002; Müller and Zank 2004)

[b]For WD stars 0050–332, 0549+158, 1254+223, 1314+293, 1615–154, 1631+781, 1634–573, 1844–233, 2004–605, 2111+498, 2211–495 (Lehner et al. 2003)

[c]Exceptions are that WD0050–332 and WD0549–158 show $Ar^0/O^0 < 1.6 \times 10^{-3}$

[d]WD stars 0050–332, 0549+158, 1254+223, 1314+293, 2004–605

the data on $N(\mathrm{C\,II}^*)$, $N(\mathrm{Mg\,II})$ and $N(\mathrm{Mg\,I})$ for the ϵ CMa line of sight lead to the result of a supersolar C abundance.

PUI and ACR data provide another source of comparison for our models. Table 1 summarizes how our model results compare with these data. We find generally good agreement,

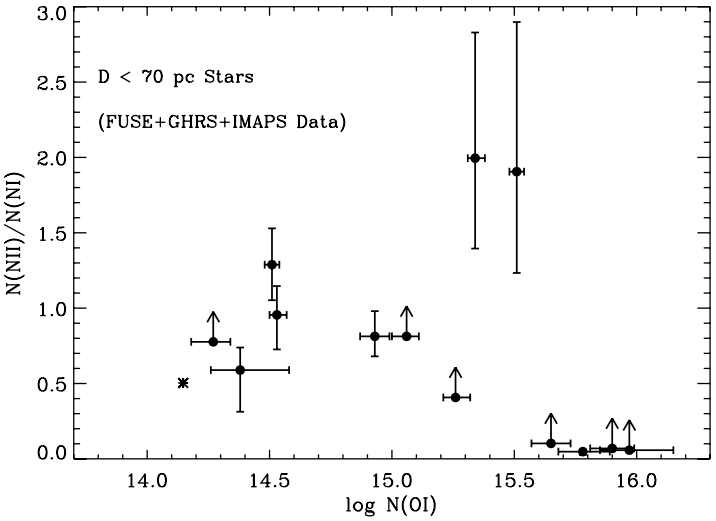

Fig. 3 FUSE, GHRS, and IMAPS data for $N(\mathrm{N\,II})/N(\mathrm{N\,I})$ versus $N(\mathrm{O\,I})$ for white dwarfs near the Sun. Also shown (*asterisk*) is the result for our photoionization models of the LIC (Model 26 from Slavin and Frisch 2007). The stars plotted are WD0050–332, WD0549+158, WD1254+223, WD1314+293, WD1615–154, WD1631+781, WD1634–573, WD1844–233, WD2004–605, WD2111+498, WD2211–495 from Lehner et al. (2003), and WD1620–391 from the FUSE archives. Data for η UMa are also plotted (Frisch et al. 2007)

though we have some indication that our assumption for the Ar abundance may be too low (we do not fix the Ar abundance in our modeling).

Looking beyond the LIC, several low column density clouds are present inside the Local Bubble. Figure 3 illustrates how the observations of O I, N I and N II toward nearby white dwarfs compares with our model results for the LIC. The column of O I should track the H I column closely since charge transfer tightly couples the ionization of the two atoms. The ratio $N(\mathrm{N\,II})/N(\mathrm{N\,I})$ is a measure of the degree of H ionization in the gas since the ionization potential of N, 14.5 eV, is close to that of H and because H and N are coupled by charge transfer. The $N(\mathrm{N\,II})/N(\mathrm{N\,I})$ ratio for our model 26 (Slavin and Frisch 2007, shown by an asterisk) is consistent with that seen toward several of the WDs. The fact that for several lines of sight this ratio is ∼0.5–1.5 illustrates that these clouds are partially ionized. Thus neither the assumptions for H II region type ionization nor those for neutral gas apply and full photoionization calculations must be carried out in order to make the ionization corrections needed to calculate elemental abundances correctly.

6 Conclusions

We have carried out detailed photoionization calculations of the LIC based on the available data on the interstellar radiation field and theoretical calculations needed to fill in gaps in that data. The combination of absorption line data toward ϵ CMa and the modeled photoionization lead us to the conclusion that the LIC has a very interesting pattern of gas phase elemental abundances. C appears to be substantially supersolar while Fe, Mg and Si are subsolar. O and N are close to solar, though perhaps slightly low. We interpret these results as indicating that carbonaceous grains have been destroyed in the LIC while silicate grains

have survived. The extra C in the gas has not been explained, but may be evidence for local enhancement of carbonaceous dust followed by grain destruction in a shock.

Acknowledgements This work has been supported by NASA grants NNG05GD36G and NNG06GE33G.

References

M. Asplund, N. Grevesse, A.J. Sauval, in *Cosmic Abundances as Records of Stellar Evolution and Nucleosynthesis*. ASP Conf. Ser., vol. 336 (2005), p. 25
A.C. Cummings, E.C. Stone, C.D. Steenberg, Astrophys. J. **578**, 194 (2002)
G.J. Ferland, K.T. Korista, D.A. Verner, J.W. Ferguson, J.B. Kingdon, E.M. Verner, PASP **110**, 761 (1998)
P.C. Frisch, J. Aufdenberg, E.B. Jenkins, C. Johns-Krull, J.D. Slavin, U.J. Sofia, D.E. Welty, D.G. York (2007, in preparation)
G. Gloeckler, L.A. Fisk (2007, this volume)
P.M. Gondhalekar, A.P. Phillips, R. Wilson, Astron. Astrophys. **85**, 272 (1980)
C. Gry, E.B. Jenkins, Astron. Astrophys. **367**, 617 (2001)
N. Lehner, E. Jenkins, C. Gry, H. Moos, P. Chayer, S. Lacour, Astrophys. J. **595**, 858 (2003)
H.-R. Müller, G.P. Zank, J. Geophys. Res. (Space Phys.) **109**, 7104 (2004)
J.D. Slavin, P.C. Frisch, Astrophys. J. **565**, 364 (2002)
J.D. Slavin, P.C. Frisch, Astrophys. J. Lett. **651**, L37 (2006)
J.D. Slavin, P.C. Frisch (2007, in preparation)
M. Witte, Astron. Astrophys. **426**, 835 (2004)